A 3D QSAR Pharmacophore Model and Quantum Chemical Structure−Activity Analysis of Chloroquine(CQ)-Resistance Reversal

Apurba K. Bhattacharjee,*,† Dennis E. Kyle,† Jonathan L. Vennerstrom,‡ and Wilbur K. Milhous†

Division of Experimental Therapeutics, Walter Reed Army Institute of Research, Silver Spring, Maryland 20910-7500, and College of Pharmacy, University of Nebraska Medical Center, 986025 Nebraska Medical Center, Omaha, Nebraska 68198-6025

Received May 2, 2002

Using CATALYST, a three-dimensional QSAR pharmacophore model for chloroquine(CQ)-resistance reversal was developed from a training set of 17 compounds. These included imipramine (**1**), desipramine (**2**), and 15 of their analogues (**3**−**17**), some of which fully reversed CQ-resistance, while others were without effect. The generated pharmacophore model indicates that two aromatic hydrophobic interaction sites on the tricyclic ring and a hydrogen bond acceptor (lipid) site at the side chain, preferably on a nitrogen atom, are necessary for potent activity. Stereoelectronic properties calculated by using AM1 semiempirical calculations were consistent with the model, particularly the electrostatic potential profiles characterized by a localized negative potential region by the side chain nitrogen atom and a large region covering the aromatic ring. The calculated data further revealed that aminoalkyl substitution at the N5-position of the heterocycle and a secondary or tertiary aliphatic aminoalkyl nitrogen atom with a two or three carbon bridge to the heteroaromatic nitrogen (N5) are required for potent "resistance reversal activity". Lowest energy conformers for **1**−**17** were determined and optimized to afford stereoelectronic properties such as molecular orbital energies, electrostatic potentials, atomic charges, proton affinities, octanol−water partition coefficients (log P), and structural parameters. For **1**−**17**, fairly good correlation exists between resistance reversal activity and intrinsic basicity of the nitrogen atom at the tricyclic ring system, frontier orbital energies, and lipophilicity. Significantly, nine out of 11 of a group of structurally diverse CQ-resistance reversal agents mapped very well on the 3D QSAR pharmacophore model.

INTRODUCTION

Development of resistance to the widely available and low cost antimalarial drug chloroquine (CQ) has significant public health implications for developing countries in malaria endemic regions.[1] The discovery[2] that verapamil could reverse CQ-resistance set in motion a substantial effort to identify other agents[3] that might also reverse CQ-resistance. Tricyclic antidepressants[4] and antihistamines[5] are two of the more well-studied drug classes examined for their potential to reverse CQ-resistance. Although little is known of the structural elements required for reversing CQ-resistance, a recent structural analysis[6] of antidepressants revealed that the direction of the dipole moment was critical to CQ-resistance reversal, an initial step in the identification of a chemical CQ-resistance reversal pharmacophore. In the present study we describe the generation of a reliable chemical function based 3D QSAR model for reversal of CQ-resistance from a comparative analysis of imipramine (**1**) and desipramine (**2**) together with 15 analogues (**3**−**17**) of these tricyclic antidepressants (Table 1). In addition we have performed several quantitative structure−activity relationship studies based on AM1 semiempirical quantum chemical calculations to assess the role of calculated stereoelectronic properties in identifying a pharmacophore model for reversal of CQ-resistance. Quantum-chemical descriptors have been frequently used in QSAR studies in recent years, because of the large well-defined physical information content encoded in many theoretical descriptors.[7]

MATERIALS AND METHODS

Procedure for Generation of the 3D QSAR Model. The three-dimensional QSAR study was performed using CATALYST 4.6 software.[8] Structures of imipramine (**1**), desipramine (**2**) and 15 analogues (**3**−**17**) of our training set were imported into CATALYST and energy minimized to the closest local minimum using the generalized CHARMM-like force field as implemented in the program. The CATALYST model treats molecular structures as templates comprising chemical functions localized in space that will bind effectively with complementary functions on the respective binding proteins. The most relevant chemical features are extracted from a small set of compounds that cover a broad range of activity.[9] Molecular flexibility is taken into account by considering each compound as an ensemble of conformers representing different accessible areas in 3D space. The "best searching procedure" was applied to select representative conformers within 20 kcal/mol from the global minimum.[10] CATALYST allows the use of structure and activity data for a set of lead compounds to create a

* Corresponding author phone: (301)319-9043; fax: (301)319-9449; e-mail: apurba.bhattacharjee@na.amedd.army.mil. Corresponding address: Department of Medicinal Chemistry, Division of Experimental Therapeutics, Walter Reed Army Institute of Research, 503 Robert Grant Avenue, Silver Spring, MD 20910.

† Walter Reed Army Institute of Research.

‡ University of Nebraska Medical Center.

10.1021/ci0200265 CCC: $22.00
Published on Web 08/02/2002

Table 1. Chemical Structures, IC_{50} Values, and Selected Molecular Properties of the Compounds

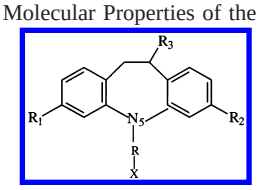

compd	R	X	R1	R2	R3	IC_{50}[a] (ng/mL)	RMI (500 ng)	log P
1 (imipramine)	-$(CH_2)_3$-	-$N(CH_3)_2$	-H	-H	-H	2.3	0.05	3.65
2 (desipramine)	-$(CH_2)_3$-	-$HNCH_3$	-H	-H	-H	2.4	0.05	2.99
3	-$CHCH_3$ $(CH_2)_2$-	-$NHCH_3$	-H	-H	-H	3.0	0.06	3.27
4 (clomipramine)	-$CHCH_3CH_2$-	-$NHCH_3$	-H	-H		4.2	0.09	3.13
5	-$(CH_2)_3$-	-$N(CH_3)_2$	-H	-Cl	-H	4.6	0.09	3.95
6	-$(CH_2)_3$-	-3 methyl piperizine	-H	-H	-H	5.2	0.11	3.01
7	-CH_2CCCH_2-	-pyrrolidine	-H	-H	-H	9.9	0.2	4.6
8	-$(CH_2)_3$-	-N methyl 1,4-diazepine	-H	-H	-H	12.2	0.25	3.28
9	-$(CH_2)_3$-	-3 methyl *N*-ethylacetyl piperizine	-H	-H	-H	15.5	0.3	2.55
10	-CH_2-	-H	-H	-H	-H	38.5	0.79	2.38
11	-$(CH_2)_3$-	-2 methyl piperizine	-H	-H	-H	43.1	0.89	2.78
12	-$COCH_2$-	-H	-H	-H	-OH	47.4	0.97	1.63
13	-$COCH_2$-	-H	-H	-H	=O	47.6	0.98	2.24
14	-$COCH_2$-	-H	-Cl	-Cl	-H	48.4	0.99	3.98
15	-$COCH_2$-	-H	-H	-H	-NH_2	49.5	1.02	1.79
16	-$COCH_2$-	-H	-H	-H	-epoxy	49.5	1.0	1.79
17	-$COCH_2$-	-H	-H	-H	-H	49.7	1.02	2.99

[a] Chloroquine plus 500 ng/mL of analogue (data shown is W2). Control IC_{50}: Indochina clone (W2) 48.7, Sierra Leone clone (D6) 2.5.

hypothesis characterizing the activity of the lead set. To obtain a reliable model adequately describing the interaction of ligands with high predictability, the CATALYST procedure recommends a collection of 15−25 chemically diverse molecules with biological activity covering 4−5 orders of magnitude for the training set.

The hypotheses are described by a set of functional features such as hydrophobic, hydrogen bond donor, hydrogen bond acceptor, and positively and negatively ionizable sites distributed over a 3D space. The hydrogen bonding features are vectors, whereas all other functions are points. The statistical relevance of the obtained hypothesis is assessed on the basis of their cost relative to the null hypothesis and their correlation coefficient.

Procedure for Semiempirical Quantum Chemical Calculations. Conformation search calculations using the "systematic search" technique via the single-point AM1 method of SPARTAN [11] was used to generate different conformers for each of the molecules. The minimum energy conformer with highest abundance (a Boltzman population density greater than 70.0%) was chosen for full geometry optimization using the AM1 algorithm.[12] The computations were carried out on a Silicon Graphics Octane workstation. To simulate physiological conditions, complete optimization of geometry was performed in the presence of an aqueous environment using the $AM1_{aq}$ method developed by Dixon et al.[13] in SPARTAN. Molecular electronic properties such as molecular orbital energies, electrostatic potentials, atomic charges, proton affinities, octanol−water partition coefficients (Log P), and structural parameters were calculated on the optimized geometry of each of the molecules using the graphics of SPARTAN. Log P was calculated using the Villar's method as implemented in SPARTAN.

Molecular electrostatic potential (MEP) maps and their electrostatic potential energy isopotential profiles were generated and sampled over the entire accessible surface of a molecule (corresponding roughly to a van der Waals contact surface). The MEP maps provide a measure of charge distribution from the point of view of an approaching reagent. However, the basis set dependence of the MEP and molecular orbital energies could not be examined due to the inadequacy of the procedure in AM1 methodology.

Biological Testing. The IC_{50} of CQ against the W2 clone of *Plasmodium falciparum* was determined in the presence and absence of 500 ng/mL of test compound.[14] The IC_{50} is the inhibitory dose or potency of a compound and is expressed as the dose that inhibits parasite growth by 50%. A RMI was calculated by dividing the IC_{50} of CQ in the presence of the tricyclic antidepressent by the IC_{50} of CQ alone. The structure/activity relationships and pharmacophore generation discussed here are based upon these activity data.

RESULTS AND DISCUSSION

3D QSAR Model for Resistance Reversal. To develop a reliable 3D QSAR model for CQ-resistance reversal, we selected a training set of 17 structurally diverse tricyclic antidepressants including imipramine (**1**) and desipramine (**2**) and 15 of their analogues, **3**−**17** (Table 1). We used IC_{50} values of CQ in the presence and absence of 500 ng/mL of the test compound as the activity parameter to develop the pharmacophore model.

The AM1 optimized structures of the compounds were imported into CATALYST from SPARTAN and were minimized to the closest local minimum using molecular mechanics (CHARMm force field). Conformational models were generated that emphasize representative coverage within a range of 20 kcal/mol above the calculated global minimum. This conformational model of the training set was used for hypothesis (pharmacophore) generation within CATALYST, which aims to identify the best three-dimensional arrangement of chemical functions explaining the activity variations among the training set. The automatic generation procedure using the HypoGen module of CATALYST was adopted for

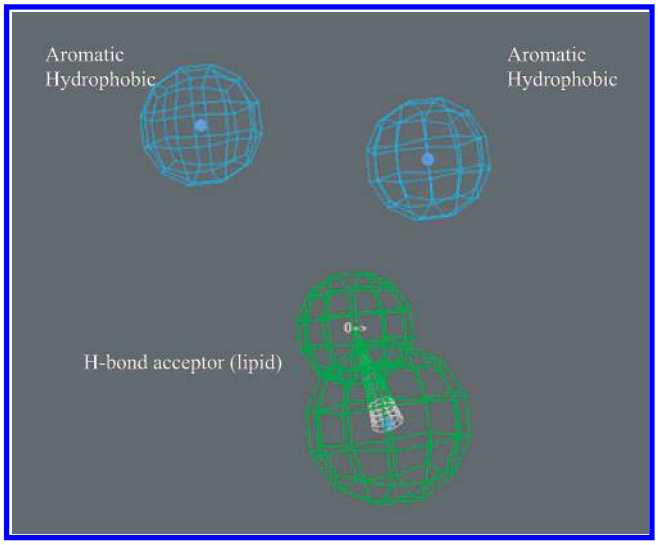

Figure 1. Pharmacophore for CQ-resistance reversal.

generation of the hypotheses. HypoGen only considers a pharmacophore that contain features with equal weights and tolerances. Each feature (e.g. hydrogen-bond acceptor, hydrogen-bond donor, hydrophobic, positive ionizable group, etc.) contributes equally to the activity estimate. Similarly, each chemical feature in the HypoGen pharmacophore requires a match to a corresponding ligand atom to be within the same distance (tolerance).[9] This method has also been documented to perform better than a structure-based pharmacophore generation.[15] In the present study, constraints were placed on the number of features such that there could be aromatic hydrophobic or aliphatic hydrophobic interactions, hydrogen bond donors, hydrogen bond acceptors, hydrogen bond acceptor (lipid), and ring aromatic sites to describe the resistance reversal activity of the compounds. During the hypothesis generation, the molecules were mapped to the pharmacophore features with their prestored conformations earlier generated using the "fast fit" techniques of CATALYST. With this backdrop, the hypothesis generation procedure generated 10 alternative pharmacophore models for the CQ-resistance reversal agents. The automatic pharmacophore generation procedure appears to perform quite well for the training set. The correlation coefficients were found to be above 0.9 for eight of the 10 models, and the RMS values ranged between 0.2 and 0.5. The total costs of the hypotheses varied over a narrow range between 68.45 and 70.54 bits. The difference between the total costs of the first and the tenth hypothesis was found to be ideally around 10 bits.[8] Significantly, the best hypothesis is characterized by one hydrogen bond acceptor (lipid) function and two aromatic hydrophobic functions (Figure 1). The estimated activity values along with the experimental IC_{50} values for resistance reversal of the compounds are presented in Table 2. Plot of the experimentally determined CQ-resistance reversal IC_{50} values versus the calculated activities demonstrates a fairly good correlation ($R = 0.97$), indicating a good predictive power of the hypothesis (Figure 2). The highly potent analogues of the series map all the functional features of the best hypothesis with high scores, whereas the less potent compounds either do not map at all or map fewer of the features. For example, **1** and **2**, the two most potent members of the series, map the hydrogen-bond acceptor (lipid) by the tertiary nitrogen atom of the side chain and

Table 2. Estimated and Experimentally Determined IC_{50} Values of CQ against W2 Clone of *Plasmodium falciparum* (in the Presence and Absence of 500 ng/mL of Test Compound) of the Compounds of the Training Set

compd	estimated IC_{50} values (ng/mL)	measured IC_{50} values (ng/mL)	error[a]
1	3.5	2.3	1.5
2	2.1	2.4	−1.1
3	2.4	3.0	−1.2
4	7.0	4.2	1.7
5	3.2	4.6	−1.4
6	6.2	5.2	1.2
7	7.6	9.9	−1.3
8	11	12.2	−1.1
9	9.3	15.5	−1.7
10	47	38.5	1.2
11	43	43.1	−1.0
12	46	47.4	−1.0
13	50	47.6	1.1
14	43	48.4	−1.1
15	43	49.5	−1.1
16	45	49.5	−1.1
17	63	49.7	1.3

[a] Error values represent the ratio of the estimated activity to its experimentally measured activity or its negative inverse if the ratio is less than one.

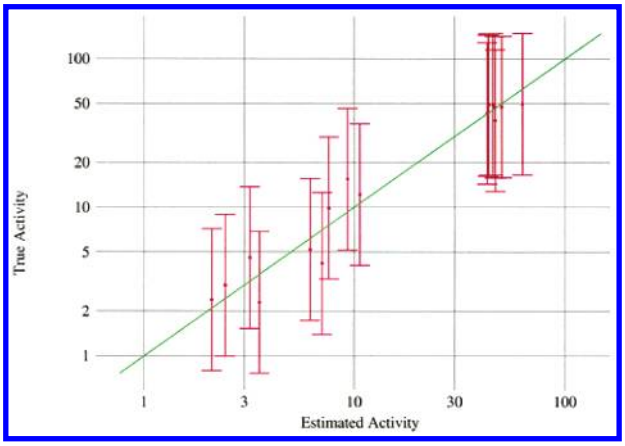

Figure 2. Correlation ($R = 0.97$) line displaying the observed versus estimated IC_{50} values (ng/mL) of the training set by using the statistically most significant hypothesis derived from the W2 activities.

the aromatic hydrophobic interactions on the two aromatic rings (Figure 3), whereas inactive analogues such as **10** and **17** do not map these features adequately (Figure 4). In the less potent analogues, despite fairly good mapping of the aromatic hydrophobic functions, the crucial hydrogen-bond acceptor (lipid) by the side chain either cannot map at all due to a lack of the side-chain nitrogen atom in the molecules or map on other atoms such as the carbonyl oxygen atom in **17** (Figure 4).

To cross-validate the pharmacophore, its features were mapped on a series of known CQ-resistance reversal agents (Chart 1) including cyproheptadine,[16] ketotefin,[16] azatadine,[16] promethazine,[17] chloropheniramine,[18] fluoxetine,[19] verapamil[2], WR 268954,[20] haloperidol,[21] amlodipine,[22] and citalopram.[23,24]

The best-fit scores and mapping of these compounds to the pharmacophore are presented in Table 3 and Figures 5 and 6. The best-fit method minimizes the conformational energy of the molecule so as to optimize the fit to the

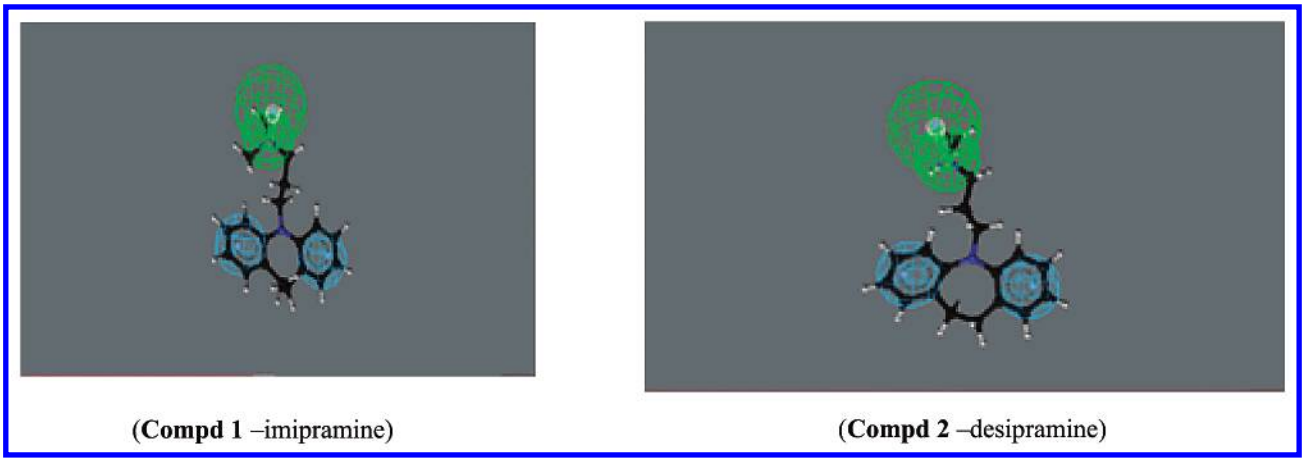

Figure 3. Mapping of the potent analogues, **1** and **2**, onto the pharmacophore model.

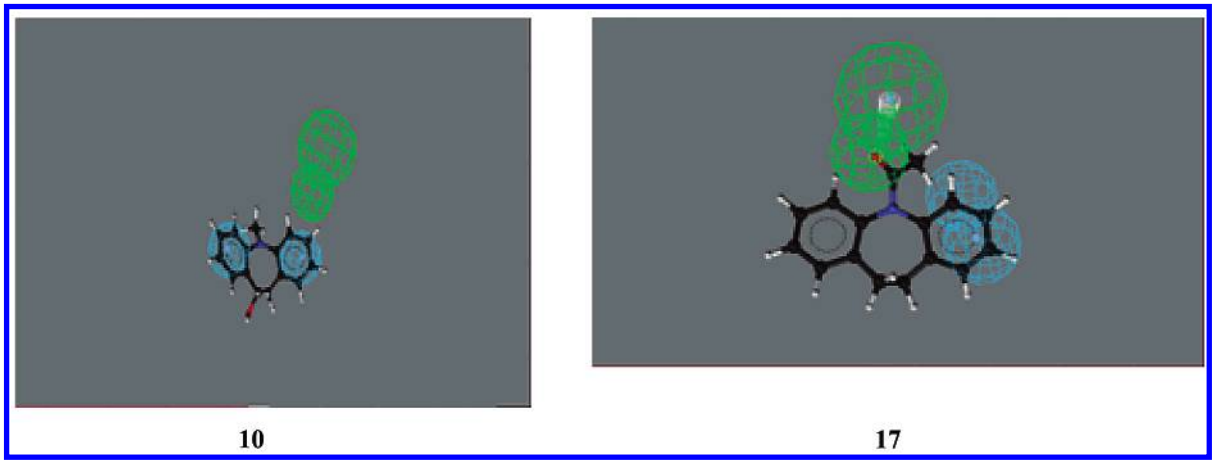

Figure 4. Mapping of the inactive analogues, **10** and **17**, onto the pharmacophore model.

Table 3. "Best-Fit" Scores of Different CQ-Resistance Reversal Agents Obtained by Mapping on the Pharmacophore Model

compd	fit score
1 (imipramine)	5.6
2 (desipramine)	5.7
cyproheptadine	4.2
ketotefin	4.5
azatadine	4.8
promethazine	4.2
chlorpheniramine	5.6
fluoxetine	5.8
verapamil	5.1
WR 268954	3.9
haloperidol	5.3
amlodipine	3.9
citalopram	5.8

pharmacophore features. The mapping of the pharmacophore on chloropheniramine, cyproheptadine, verapamil, and haloperidol is shown in Figure 5 and on promethazine, fluoxetine, WR 268954, and amlodipine in Figure 6. Except for WR 268954 and amlodipine, the pharmacophore maps on all these compounds on two aromatic hydrophobic regions and a hydrogen-bond acceptor site (Figure 6). In WR 268954, although the H-bond acceptor function maps well in the side chain nitrogen atom, only one of the two aromatic hydrophobic functions maps on the lone aromatic ring and the other maps on a methyl substituent in the aromatic ring of the molecule. Similarly, in amlodipine, one aromatic hydrophobic function maps on the only phenyl ring, not in the dihydropyridine ring and the second hydrophobic function does not map at all; the H-bond acceptor function maps on an oxygen atom (Figure 6). Perhaps due to these discrepancies in the pharmacophore maps both these two compounds are not as potent CQ-resistance reversal agents as the others.[20,21] The best-fit score for both the compounds is also the lowest (3.9) among the set of CQ-resistant reversal agents (Table 3 and Chart 1). The best-fit values for the remaining CQ-resistance reversal agents range between 4.1 and 5.8 and show excellent agreement with the pharmacophore model (Table 3). For comparison, the fit values for **1** and **2** are 5.6 and 5.7, respectively. Thus, clearly two hydrophobic aromatic regions and a hydrogen-bond acceptor (lipid) center, preferably on a nitrogen atom, are necessary for potent CQ-resistance reversal activity.

By using this pharmacophore model as a search template we have performed a database search for potential new CQ-reversal agents from our in-house Chemical Information System [25] database of over 240 000 compounds. This procedure has identified few quinazolinesulfonalide analogues as promising candidates for further studies. The Chemical Information System database was transformed into a multiconformer database in CATALYST using the catDB utility program as implemented in the software. The catDB format allows a molecule to be represented by a limited set of conformations thereby permitting conformational flexibility to be included during the search of the database.

Quantum Chemical Calculations. The calculated stereoelectronic properties of the compounds in the gas phase (in vacuo) paralleled the aqueous phase results. Since the

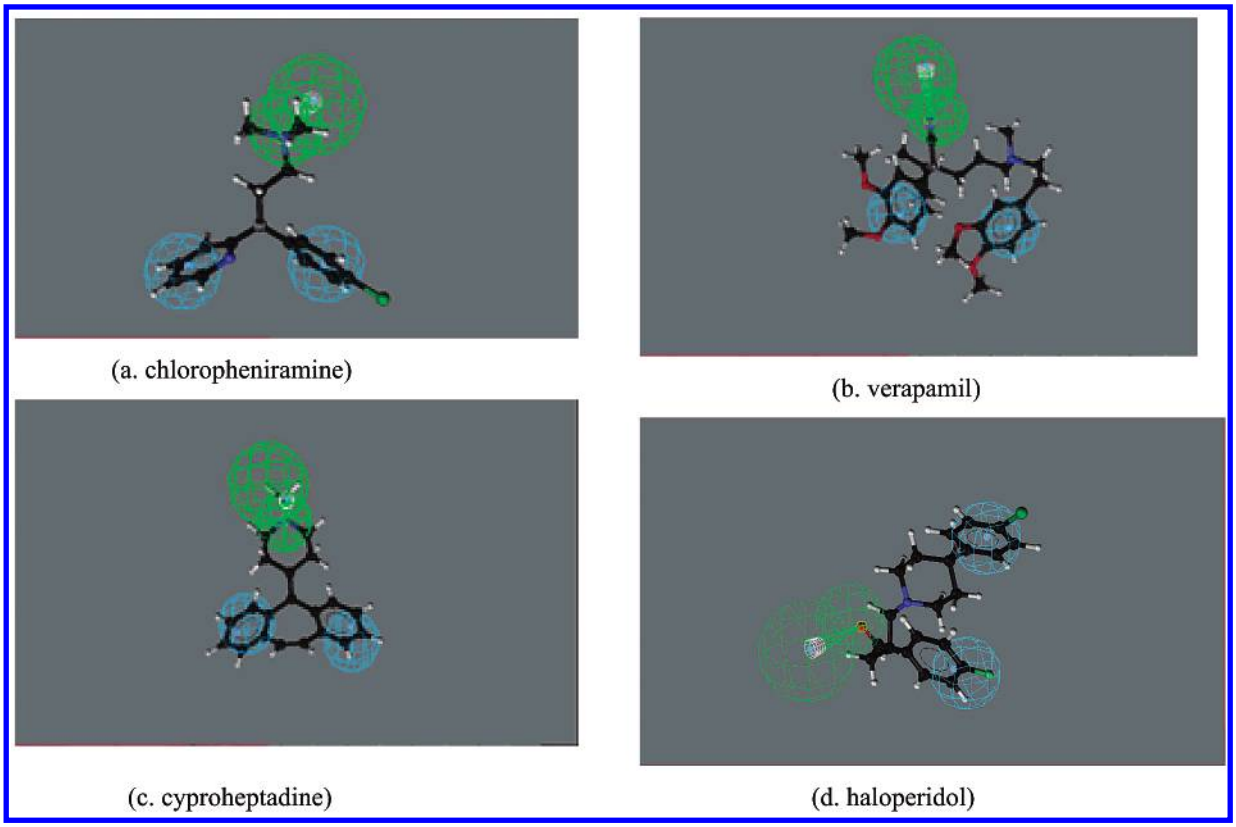

Figure 5. Mapping of the pharmacophore in four well-known CQ-resistance reversal agents: (a) chloropheniramine, (b) verapamil, (c) cyproheptadine, and (d) haloperidol.

Chart 1. Structures of Known CQ-Resistance Reversal Agents That Were Mapped in the Pharmacophore

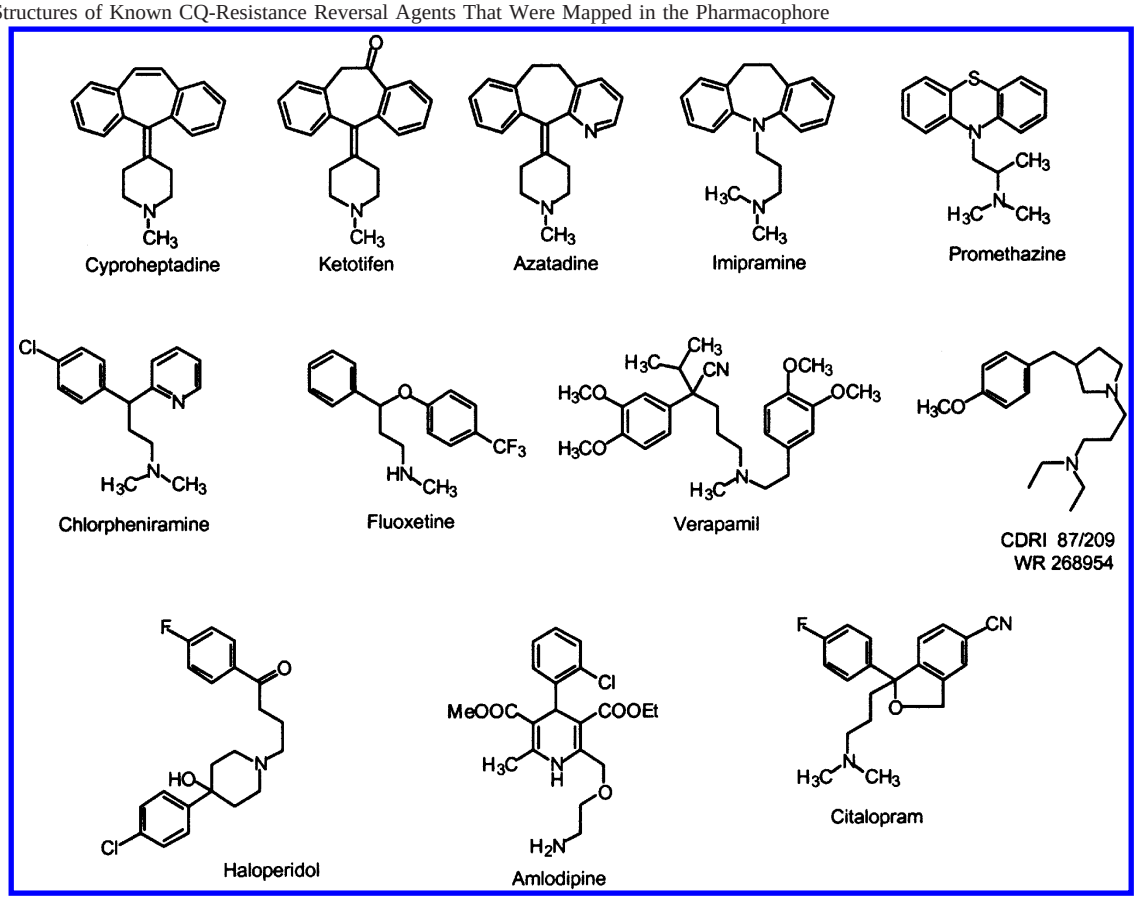

aqueous phase results better simulate the biological environment, the stereoelectronic properties presented here are based on results obtained from AM1-aqueous calculations on the optimized geometry of the molecules (Tables 1 and 4). The

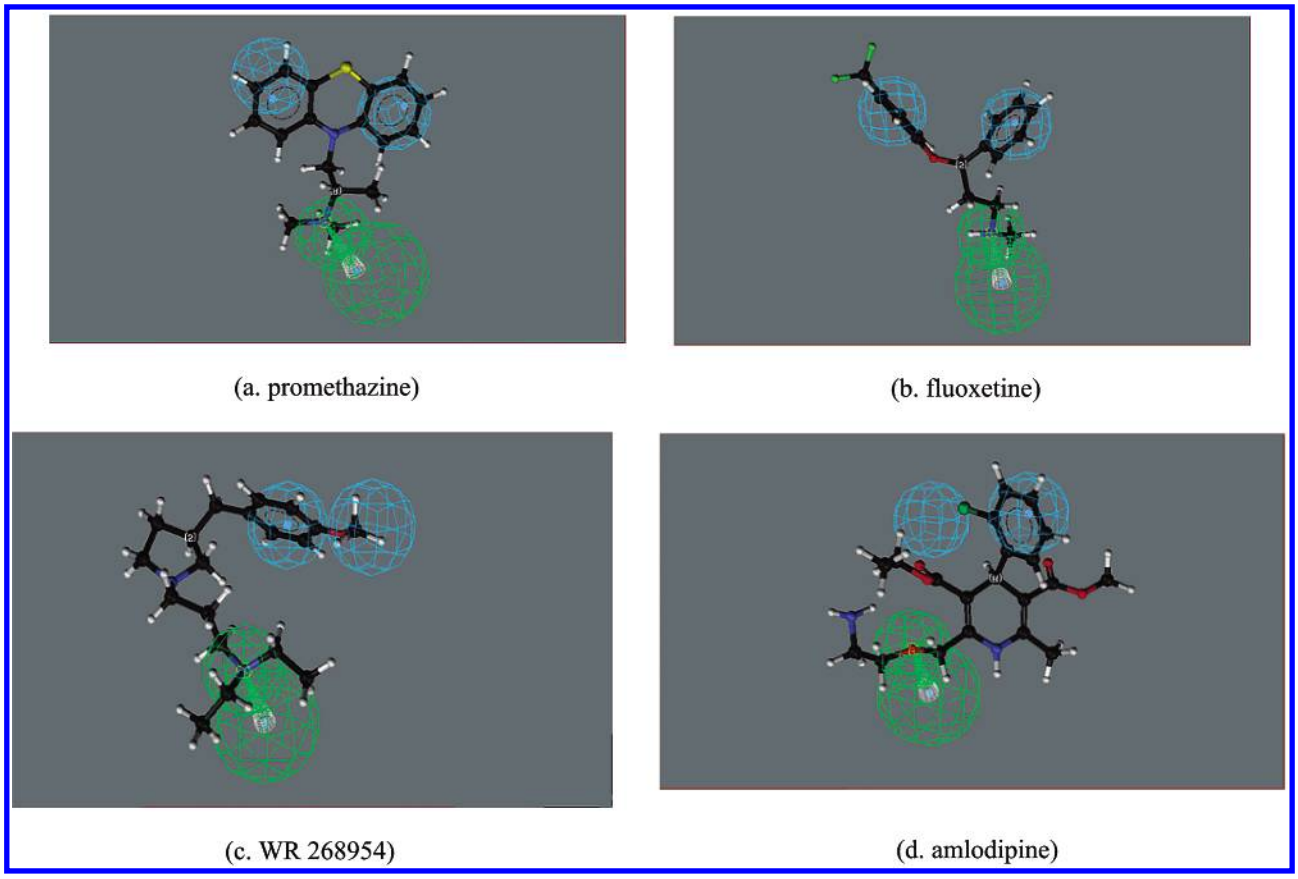

Figure 6. Mapping of the pharmacophore in (a) promethazine, (b) fluoxetine, (c) WR 268954, and (d) amlodipine*. *Part (d) shows the inadequacy in the mapping of the hydrophobic function in the molecule.

results are analyzed on the basis of the following two attributes:

Steric Attributes. Inspection of the RMI activity profile and the structure of the compounds (Table 1) indicates that the more potent analogues of the series have a secondary or tertiary aliphatic aminoalkyl nitrogen atom with a two or three carbon bridge in the side chain joined to the heteroaromatic nitrogen (N5) atom. This appears to be an important structural requirement for resistance reversal ability of the compounds since compounds without this nitrogen atom do not seem to have potent resistance reversal ability. Structural parameters such as bond lengths, valence angles, and dihedral angles of the heterocycle aromatic moiety in the optimized geometry of the analogues do not show any noticeable difference between the less potent and the more potent analogues (data not shown). The nonbonded distance between the N5 atom of the heterocyclic ring and the side chain nitrogen atom ranged from 3.3 to 5.9 Å for the 10 nitrogen containing side-chain analogues. However, no correlation was observed between this N−N distance (minimum or maximum) and the experimental RMI values.

Electronic Attributes. Increase in intrinsic nucleophilicity or basicity of the N5 nitrogen atom in the heterocyclic moiety appears to be significantly related to potent resistance reversal activity of the compounds. Both calculated proton affinity (PA) of the N5 atom and negative potential by the N5 atom in the compounds support this view (Table 4). Increasing PA of the N5 atom correlated well with reversal activity (Figure 7) ($A = 219.7-0.31\ IC_{50}$, $R = 0.8068$). PA is a theoretical measure of basicity of a specific site in the molecule. It is calculated as the difference in energy between the protonated and nonprotonated form of electronic lone pair of the proton acceptor atoms of the molecule after a geometrical optimization.[26,27]

Table 4. Selected Stereoelectronic Properties and IC_{50} Values of the Compounds

compd	proton affinity (PA) (kcal/mol)	HOMO (in eV)	LUMO (in eV)	MEP (N5) (kcal/mol)	IC_{50}[a] (ng/mL)	RMI (500 ng)
1	214.5	−8.28	0.42	−41.5	2.3	0.05
2	217.6	−8.2	0.5	−40.9	2.4	0.05
3	224.6	−8.25	0.52	−41.5	3.0	0.06
4	221.2	−8.23	0.46	−30.1	4.2	0.09
5	211.6	−8.44	0.2	−37.8	4.6	0.09
6	215.3	−8.30	0.45	−40.2	5.2	0.11
7	221.3	−8.26	0.44	−43.0	9.9	0.2
8	216.7	−8.27	0.47	−40.3	12.2	0.25
9	214.3	−8.36	0.40	−38.8	15.5	0.3
10	215.4	−8.5	0.39	−45.2	38.5	0.79
11	215.3	−8.3	0.43	−40.2	43.1	0.89
12	205.9	−8.87	−0.07	−17.6	47.4	0.97
13	198.1	−9.2	−0.43	−9.6	47.6	0.98
14	200.4	−9.1	−0.32	−12.5	48.4	0.99
15	200.0	−9.0	0.01	−16.0	49.5	1.02
16	204.3	−9.0	−0.18	−13.6	49.5	1.0
17	205.3	−8.84	0.06	−19.2	49.7	1.02

[a] Chloroquine plus 500 ng/mL of analogue (data shown is W2). Control IC_{50}: Indochina clone (W2) 48.7, Sierra Leone clone (D6) 2.5.

Another measure of basicity, the negative electrostatic potential (MEP) values by the N5 atom, was found to be more negative in the more potent analogues (Table 4). The magnitude of negative electrostatic potential by an atom on the van der Waals contact surface of the molecule is a measure of intrinsic nucleophilicity or basicity of the atom

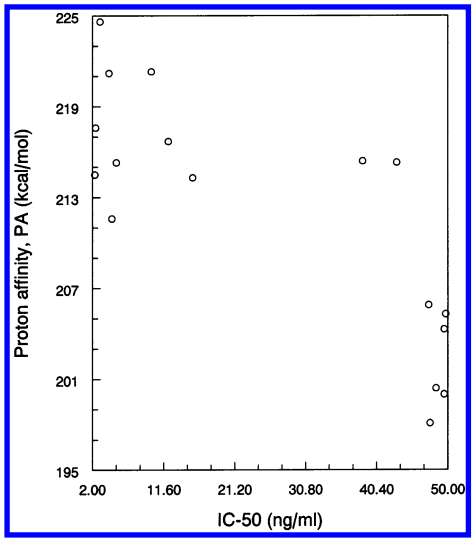

Figure 7. CQ-resistance reversal activity (ng/mL) versus proton affinity (PA) in kcal/mol of the compounds.

as it identifies the electron density of a region in the molecule.[28] A majority of the more potent members of the series have a negative potential by the N5 atom more negative than −30.0 kcal/mol and a proton affinity greater than 210.0 kcal/mol, respectively (Table 4). The three-dimensional electrostatic potential profiles beyond the van der Waals surface of the molecules at −40.0 kcal/mol (Figure 8) clearly support this observation as the more potent compounds (**1**−**9**) with IC_{50} values in the range 2.3−15.5 nM all have a distinct localized negative potential region by the N5 atom.

In another three-dimensional representation of electrostatic potential profiles beyond the van der Waals surface at −10.0 kcal/mol (Figure 9) the more potent compounds (**1**−**9)** show a large extended potential region over the aromatic heterocyclic ring in addition to the localized negative potential region by the terminal side chain N atom. This feature indicates a probable role of the aromatic π electrons in the activity of the analogues as these characteristics are mostly absent in the less potent analogues. In the less potent analogues **(10**−**17)**, the region near the terminal side chain N atom is either absent or extensively delocalized. The localized electrostatic region by the terminal side chain nitrogen atom may work as a powerful recognition site of the potent analogues that may enable them to form hydrogen bonds with the complimentary sites in the receptor molecules. Electrostatic potential characteristics are considered to be key features of molecules through which it recognizes its receptor

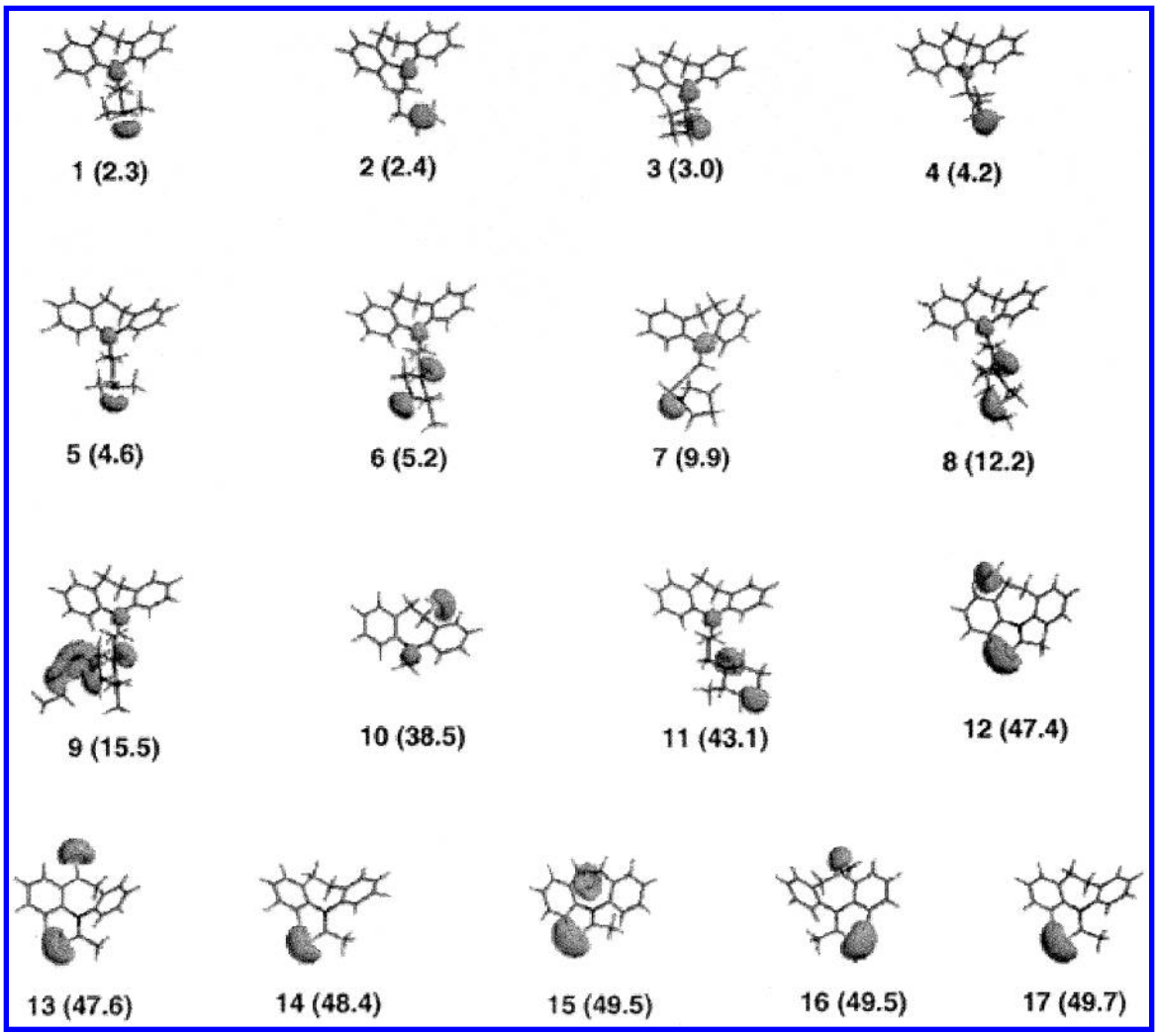

Figure 8. Three-dimensional electrostatic potential profiles at −40 kcal/mol of the compounds indicating the characteristic localized negative potential regions by the N5 atom of the tricyclic ring and the side chain nitrogen atom in the more potent analogues. Values in parentheses indicate IC_{50} of CQ plus 500 ng/mL of analogue in W2.

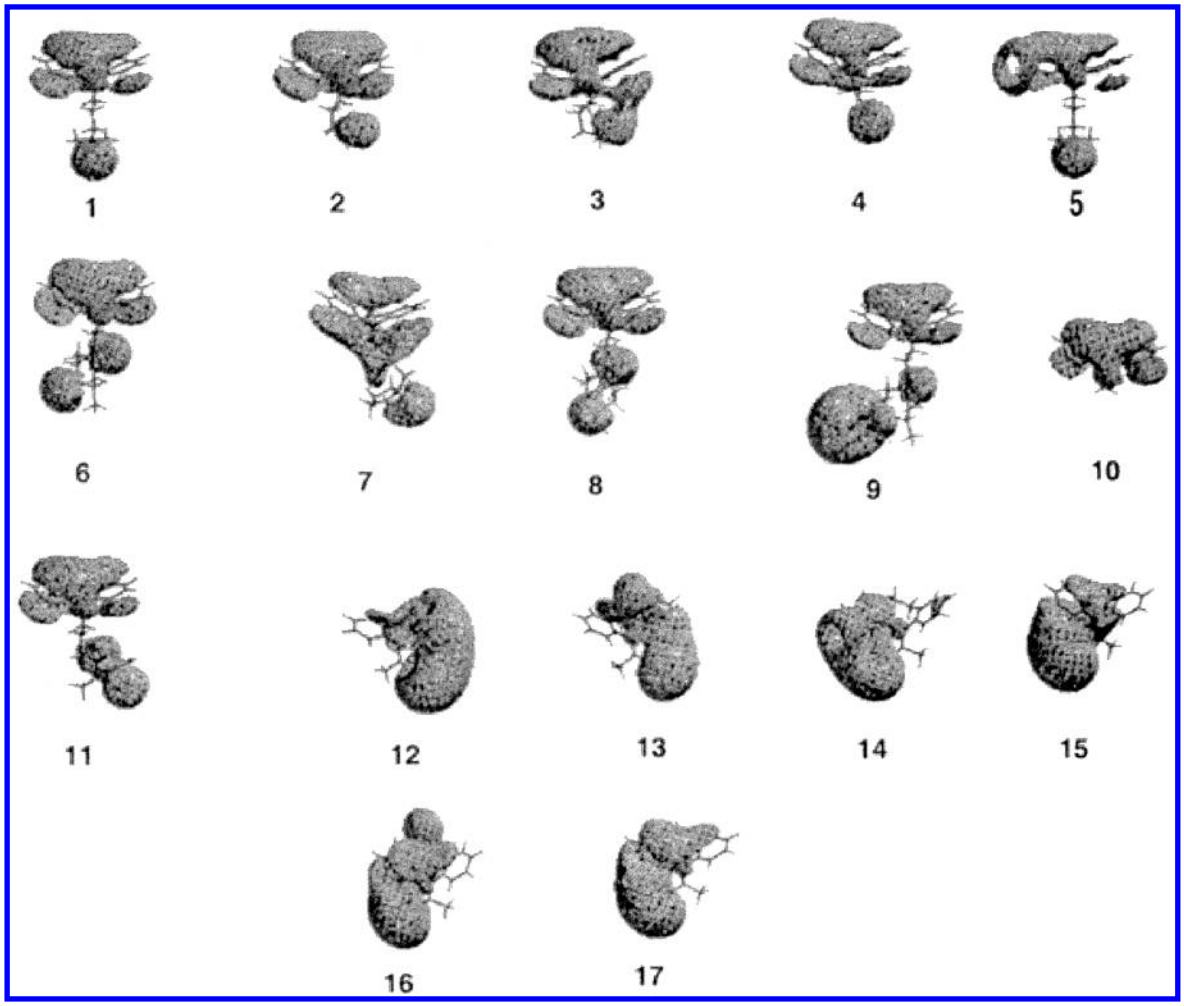

Figure 9. Three-dimensional electrostatic potential profiles at −10 kcal/mol of the compounds showing the negative potential cover of the tricyclic aromatic ring in the more potent analogs.

at longer distances and thus promotes interaction between them.[29] Therefore, the electrostatic potential features are consistent with the pharmacophore model generated in the CATALYST where the hydrogen bond acceptor site is found at the side chain nitrogen atom and the aromatic hydrophobic regions by the heterocyclic aromatic rings. We have recently proposed[6] a model for electronic bioisosterism and a common pharmacophore from the observed similarity of MEP profiles and a common structural framework of the three antihistamines cyproheptadine, azatadine and chloropheniramine and two tricyclic antidepressants imipramine and desipramine. Thus, a common pharmacophoric pattern for all these compounds for potent resistance reversal activity cannot be ruled out. The observation that the calculated dipole moment vectors pointing toward the aromatic ring or the nitrogen atom of the tricyclic ring in the potent analogues supports the important role of the aromatic ring toward activity.

Inspection of variations in the molecular orbital energies indicates that electron exchange and electron-transfer ability of the compounds may have a role in CQ-resistance reversal activity. Highest occupied molecular orbital (HOMO) and the lowest unoccupied molecular orbital (LUMO) energies (Table 3) show that less active analogues have more negative HOMO and near zero to negative LUMO energies. Plots of both HOMO and LUMO energies against IC_{50} values show fairly linear trends ($A = -8.2-0.01\ IC_{50}$, $R = 0.8543$) for the HOMO energies and ($A = 0.52-0.01\ IC_{50}$, $R = 0.7738$) for the LUMO energies, respectively. The least active analogues had HOMO energy values more negative than −8.80 eV and the LUMO energies less than 0.01 eV to negative values. Thus, the two frontier orbital energies clearly indicate an important role of charge-transfer interactions with the binding site in the receptor for potent activity. Electron donating or withdrawing groups in the compounds may be responsible for an increase or decrease in the orbital energies by allowing modulation of the molecular electronic "band gaps".[30]

Empirical Structure−Activity Relationships. Relationship between activity and certain physicochemical properties based on empirical calculations may also provide valuable structure−activity information. One important physicochemical property is the study of lipophilicity of the compounds since it is directly related with the transport of the drug to the biologically active site. Although there is no experimental standard procedure to determine this property, the most commonly used method is the logarithm of distribution coefficient of the solubilities in *n*-octanol/water phases. Because of a lack of experimental data on lipophilicity of the present compounds, we have calculated the log P, the lipophilicity index using the Villars scale as implemented in SPARTAN.[11] A plot of calculated log P versus IC_{50} values shows a near linear correlation ($A = 3.52-0.02\ IC_{50}$, $R = 0.828$) where activity is found to increase with increasing lipophilicity. Therefore, the lipophilicity of the compounds

may be an important factor associated with CQ-resistance reversal. This observation is consistent with the hydrophobic sites in the CQ-resistance reversal pharmaocophore model generated by CATALYST.

CONCLUSION

The CATALYST 3D-QSAR model of CQ-resistance reversal based on tricyclic antidepressants **1**−**17** could fairly well correlate between estimated and experimentally determined activities. Significantly, nine out of 11 of a group of structurally diverse CQ-resistance reversal agents mapped very well on the 3D QSAR pharmacophore model.

Two aromatic hydrophobic sites and a hydrogen bond acceptor site, preferably at a side chain nitrogen atom, appear to be necessary for potent resistance reversal activity. QSAR studies based on calculated quantum chemical descriptors also yielded a satisfactory correlation between CQ-resistance reversal activity and certain electronic properties such as the frontier orbital energies and the intrinsic basicity of the nitrogen atom in the tricyclic heterocycle. The electrostatic potential profiles, characterized by a localized negative potential region by the side chain nitrogen atom and a large region covering the aromatic ring, clearly seem to associate potent CQ-resistance reversal activity. The 3D QSAR pharmacophore model appears to be consistent with this observation. Empirical structure−activity studies showed a good correlation between CQ-resistance reversal activity and lipophilicity and density of the molecules. Since both frontier HOMO and LUMO orbital energies and log P parameters correlate well with activity, charge-transfer interactions with the hydrophobic binding site at the receptor may contribute to the mechanism of CQ-resistance reversal. In summary, since the identity of the CQ-resistance reversal target is still unknown, this three-dimensional QSAR pharmacophore model should aid in the design of well-tolerated compounds with specificity as CQ-resistance reversal agents.

REFERENCES AND NOTES

(1) Trigg, P. I.; Kondrachine, A. V. In *Malaria, Parasite Biology, Pathogenesis, and Protection*; Sherman, I. W., Ed.; ASM Press: Washington, DC, 1998; Chapter 2, pp 11−22.
(2) Martin, S. K.; Oduola, A. M. J.; Milhous, W. K. Reversal of chloroquine resistance in *Plasmodium falciparum* by verapamil. *Science* **1987**, *235*, 899−901.
(3) Milhous, W. K.; Kyle, D. E. In *Malaria, Parasite Biology, Pathogenesis, and Protection*; Sherman, I. W., Ed.; ASM Press: Washington, DC, 1998; Chapter 21, pp 303−316.
(4) Basco, L. K.; LeBras, J. Reversal of chloroquine resistance with desipramine in isolates of *Plasmodium falciparum* from Central and West Africa. *Trans. R. Soc. Trop. Med. Hyg.* **1990**, *84*, 479−481.
(5) Basco, L. K.; Ringwald, P.; LeBras, J. Chlroquine potentiating action of antihistaminics in *Plasmodium falciparum* in vitro. *Ann. Trop. Med. Parasitol.* **1991**, *85*, 223−228.
(6) Bhattacharjee, A. K.; Kyle, D. E.; Vennerstrom, J. L. Structural analysis of chloroquine resistance reversal in imipramine analogues. *Antimicrob. Agents Chemother*. **2001**, *45*, 2655−2657.
(7) Karelson, M.; Lobanov, V. S. Quantum chemical descriptors in QSAR/QSPR studies. *Chem. Rev.* **1996**, *96*, 1027−1043, and references therein.
(8) CATALYST Version 4.6; Accelrys Inc.: San Diego, CA, 2001.
(9) *Pharmacophore, Perception, Development, and Use in Drug Design*; Guner, O. F., Ed.; International University Line Biotechnology Series, La Jolla, CA, 2000; Chapter 26, pp 501−511.
(10) Smellie, A.; Teig, S. L.; Towbin, P. J. Poling: promoting conformational variation. *J. Comput. Chem*. **1995**, *16*, 171−187.
(11) *SPARTAN* version 5.1, Wavefunction, Inc., 18401 Von Karman Ave., #370, Irvine, CA 92715.
(12) Dewar, M. J. S.; Zoebisch, E. G.; Horsley, E. F.; Stewart, J. J. P. A new general purpose quantum mechanical molecular model. *J. Am. Chem. Soc.* **1985**, *107*, 3902−3909.
(13) Dixon, R. W.; Leonard, J. M.; Hehre, W. J. A. A. continuum solvation model for the AM1 semiempirical method. *Isr. J. Chem.* **1993**, *33*, 427−434.
(14) Kyle, D. E.; Oduola, A. M. J.; Martin, S. K.; Milhous, W. K. *Plasmodium falciparum* modulation by calcium antagonists of resistance to chloroquine, desethylchloroquine, quinine, and quinidine in vitro. *Trans. R. Soc. Trop. Med. Hyg.* **1990**, *84*, 474−478.
(15) Greenridge, P. A.; Weiser, J. A comparison of methods for pharmacophore generation with the catalyst software and their use for 3D-QSAR: Application to a set of 4-aminopyridine thrombin inhibitors. *Mini Rev. Med. Chem.* **2001**, *1*, 79−87.
(16) Peters, W.; Ekong, R.; Robinson, B. L.; Warhurst, D. C. The chemotherapy of rodent malaria. XLV. Reversal of chloroquine resistance in rodent and human *Plasmodium* by antihistaminic agents. *Ann. Trop. Med. Parasitol.* **1990**, *84*, 541−551.
(17) Oduola, A.; Sowunmi, A.; Milhous, W.; Brewer, T.; Kyle, D.; Gerena, L.; Rossan, R.; Salako, L.; Schuster, B. In vitro and in vivo reversal of chloroquine resistance in *Plasmodium falciparum* with promethazine. *Am. J. Trop. Med. Hyg.* **1998**, *58*, 625−629.
(18) Sowunmi, A.; Oduola. A. M. Comparative efficacy of chloroquine/chloropheniramine combination and mefloquine in treatment of chloroquine resistant *Plasmodium falciparum* in Nigerian children. *J. Trans. R. Soc. Trop. Med. Hyg*. **1997**, *91*, 689−693.
(19) Gerena, L.; Bass, S.; Kyle, D. E.; Oduola, A. M.; Milhous, W. K.; Martin, R. K. Fluoxetine hydrochloride enhances in vitro susceptibility to chloroquine in resistant *Plasmodium falciparum*. *Antimicrob. Agents Chemother*. **1992**, *36*, 2761−2765.
(20) De, D.; Bhaduri, A. P.; Milhous, W. K. Circumvention of chloroquine resistance by WR268954, a newly synthesized reversal modulator. *Am. J. Trop. Med. Hyg*. **1993**, *49*, 113−120.
(21) Kyle, D. E. et al., unpublished results.
(22) Deloron, P.; Basco, L. K.; Dubois, B.; Gaudin, C.; Clavier, F.; Le Bras, J.; Verdier, F. In vitro and in vivo potentiation of chloroquine against malaria parasite by an enantiomer of amlodipine. *Antimicrob. Agents Chemother*. **1991**, *35*, 1338−1342.
(23) Evans, S. G.; Butkow, N.; Stilwell, C.; Berk, M.; Kirchmann, N.; Havlik, I. Citalopram enhances the activity of chloroquine in resistant *Plasmodium in vitro* and in vivo. *J. Pharmacol. Exp. Ther.* **1998**, *286*, 172−174.
(24) Taylor, D.; Walden, J. C.; Robins, A. H.; Smith, P. J. Role of the neurotransmitter reuptake-blocking activity of antidepressants in reversing chloroquine resistance in vitro in *Plasmodium falciparum*. *Antimicrob. Agents Chemother*. **2000**, *44*, 2689−2692.
(25) Archives of the Chemical Information System, Division of Experimental Therapeutics, Walter reed Army Institute of Research, Silver Spring, MD; Data Sheet No: AW41724.
(26) Dewar, M. J. S.; Dieter, K. M. Evaluation of AM1 calculated proton affinities and deprotonation enthalpies. *J. Am. Chem. Soc*. **1986**, *108*, 8075−8086.
(27) Lopez-Romero, B.; Evrard, G.; Durant, F.; Sevrin, M.; George, P. Molecular structure and stereoelectronic properties of sarmazenil − a weak inverse agonist at the omega modulatory sites (benzodiazepine receptors): comparison with bretazenil anf flumazenil. *Bioorg. Med. Chem*. **1998**, *6*, 1745−1757.
(28) Orozco, M.; Luque, F. J. In *Molecular Electrostatic Potential. Concepts and Applications. Theoretical and Computational Chemistry*; Murray, J. S., Sen, K., Eds.; Elsevier Science B.V.: Amsterdam, 1996; Vol. 3, pp 181−218.
(29) Murray, J. S.; Zilles, B. A.; Jayasuriya, K.; Politzer, P. Comparative analysis of the electrostatic potentials of dibenzofuran and some dibenzo-p-dioxins. *J. Am Chem. Soc*. **1986**, *108*, 915−918.
(30) Pearson, R. G. The principle of maximum hardness. *Acc. Chem. Res*. **1993**, *26*, 250−255.

CI0200265